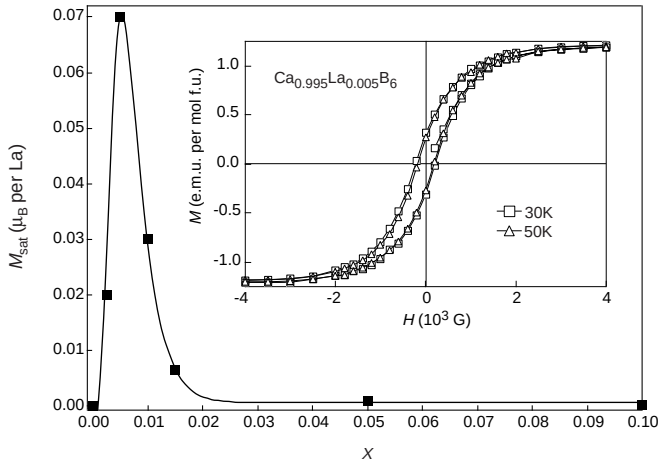

Figure 3 Saturation moment at $T = 5$ K per mol La as a function of La concentration in CaB_6. The line is a guide to the eye. Inset, hysteresis loops at 30 K and 50 K for $Ca_{0.995}La_{0.005}B_6$.

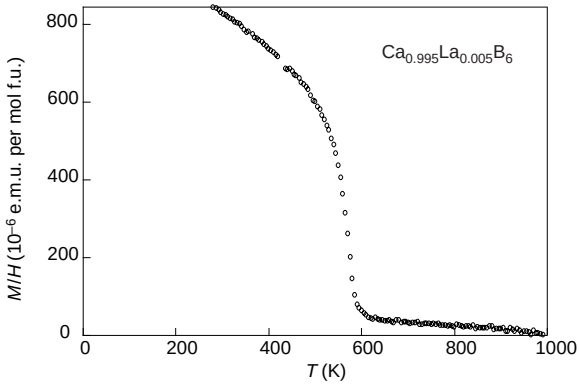

Figure 4 Magnetization of $Ca_{0.995}La_{0.005}B_6$ in a fixed applied field of 0.1 T as a function of temperature. These data were measured using a Faraday balance magnetometer.

carrier doping on the basis of the band structure of the alkaline-earth hexaborides. Calculations[10] show that the details of the overlap of valence and conduction bands at the X-point of the Brillouin zone depend sensitively on the crystallographic parameter fixing the location of the borons in the unit cell; this parameter determines the relative length of the inter- and intra-octahedral boron–boron bonds. Even small changes in this parameter in the calculations alter the behaviour from insulating to metallic. So we might expect vacancies and foreign-atom additions to alter significantly the properties of the divalent hexaborides for very small dopings, such as seen in materials with similar band structure features (for example, grey tin and bismuth).

Two suggestions for the origin of the weak ferromagnetism which we have observed are (1) ordered defect moments and (2) ferromagnetic polarization of the low-density electron gas. Because no obvious source for a strong coupling giving rise to a Curie temperature as high as $T_C = 600$ K presents itself, the coupling of magnetic moments localized on the La or other unspecified impurities on this scale seems rather implausible. A more likely candidate for the origin of the magnetic polarization emerges from studies of electronic correlations in the low-density electron gas, such as those of Ceperley and Alder[11]. This is a topic of theoretical speculation with a long history, going back to Block and Wigner[1]. The study of Ceperley and Alder is a $T = 0$ K computation, comparing unpolarized and completely polarized states of the electron gas, with ferromagnetism showing up for values of r_S of the order 80 a_B. (Here r_S is the radius of the sphere containing one conduction electron; a_B the Bohr radius.) Later calculations have lowered this value to ~20 a_B (ref. 12). For $x = 0.005$, we compute $r_S = 15.0$ Å $= 28.4\, a_B$, using the Bohr radius for the free electron. A recent calculation by Ortiz, Harris and Ballone[13] treating partially spin-polarized states of the low-density electron gas has, in fact, found evidence that near $r_S = 30\, a_B$ the stable state is one with ferromagnetic polarization of the order of 10%; this is essentially our experimental finding of an ordered moment of ~0.07 μ_B per carrier at $x = 0.005$. The natural energy scale here is the Fermi energy, E_F; for free electrons we have $E_F = 0.062$ eV $= 720$ K for $x = 0.005$ in CaB_6, of the order of the observed Curie temperature.

The ferromagnetic ground state of a dilute, three-dimensional electron gas has not previously been reported experimentally. But such a ground state seems to provide a possible description of the weak ferromagnetism reported here, although the temperature scale of the phenomenon is unexpected. Detailed calculations appropriate to the lattice case at finite temperature are clearly needed, as is much further experimental elaboration of the details of this ferromagnetism. □

Received 14 July; accepted 4 November 1998.

1. Herring, C. *Magnetism* Vol. IV (eds Rado, G. T. & Suhl, H.) Ch. 2 (Academic, New York, 1966).
2. Schmidt, P. H. *et al.* Anisotropy of thermionic electron emission values for LaB_6 single-crystal emitter cathodes. *Appl. Phys. Lett.* **29,** 400–410 (1976).
3. Lafferty, J. M. *J. Appl. Phys.* **22,** 299–301 (1951).
4. Erkelens, W. A. C. *et al.* Neutron scattering study of the antiferroquadrupolar ordering in CeB_6 and $Ce_{0.75}La_{0.25}B_6$. *J. Magn. Magnet Mater.* **63/64,** 61–63 (1987).
5. Nyhus, P., Cooper, S. L., Fisk, Z. & Sarrao, J. L. Low-energy excitations of the correlation-tap insulator SmB_6. *Phys. Rev. B* **55,** 12488–12496 (1997).
6. Süllow, S. *et al.* Structure and magnetic order of EuB_6. *Phys. Rev. B* **57,** 5860–5869 (1998).
7. Degiorgi, L., Felder, E., Ott, H. R., Sarrao, J. L. & Fisk, Z. Low-temperature anomalies and ferromagnetism in EuB_6. *Phys. Rev. Lett.* **79,** 5134–5137 (1997).
8. Longuet-Higgins, H. C. & Roberts, M. de V. The electronic structure of the borides MB_6. *Proc. R. Soc. Lond. A* **224,** 336–347 (1954).
9. Ott, H. R. *et al.* Structure and electronic properties of SrB_6. *Z. Phys. B* **102,** 337–345 (1997).
10. Massida, S., Continenza, A., de Pascale, T. M. & Monnier, R. Z. Electronic structure of divalent hexaborides. *Z. Phys. B* **102,** 83–89 (1997).
11. Ceperley, D. M. & Alder, B. J. Ground state of the electron gas by a stochastic method. *Phys. Rev. Lett.* **45,** 566–569 (1980).
12. Alder, B. J., Ceperley, D. M. & Pollock, E. L. *Int. J. Quantum Chem. Symp.* **16,** 49–61 (1982).
13. Ortiz, G., Harris, M. & Ballone, P. cond-mat/9810126.

Acknowledgements. Z.F. thanks E. Abrahams, G. Aeppli, L. Gor'kov, P. Kumar, E. Manousakis, G. Ortiz and D. Pines for discussions. Work at NHMFL was supported by the NSF; work at Los Alamos was done under the auspices of the US Department of Energy; and the work at ETH Zürich was supported by the Schweizerische Nationalfonds zur Förderung der wissenschaftlichen Forschung.

Correspondence and requests for materials should be addressed to Z.F. (e-mail: fisk@magnet.fsu.edu).

Improved quantum efficiency for electroluminescence in semiconducting polymers

Yong Cao, Ian D. Parker, Gang Yu, Chi Zhang & Alan J. Heeger

UNIAX Corporation, 6780 Cortona Drive, Santa Barbara, California 93117-3022, USA

Some conjugated polymers have luminescence properties that are potentially useful for applications such as light-emitting diodes, whose performance is ultimately limited by the maximum quantum efficiency theoretically attainable for electroluminescence[1,2]. If the lowest-energy excited states are strongly bound excitons (electron–hole pairs in singlet or triplet spin states), this theoretical upper limit is only 25% of the corresponding quantum

efficiency for photoluminescence: an electron in the π*-band and a hole (or missing electron) in the π-band can form a triplet with spin multiplicity of three, or a singlet with spin multiplicity of one, but only the singlet will decay radiatively[3]. But if the electron–hole binding energy is sufficiently weak, the ratio of the maximum quantum efficiencies for electroluminescence and photoluminescence can theoretically approach unity. Here we report a value of ~50% for the ratio of these efficiencies (electroluminescence:photoluminescence) in polymer light-emitting diodes, attained by blending electron transport materials with the conjugated polymer to improve the injection of electrons. This value significantly exceeds the theoretical limit for strongly bound singlet and triplet excitons, assuming they comprise the lowest-energy excited states. Our results imply that the exciton binding energy is weak, or that singlet bound states are formed with higher probability than triplets.

The devices for the electroluminescence (EL) and photoluminescence (PL) measurements were fabricated in the thin sandwich configuration: anode/polymer/cathode. The electronic structure of alkoxy derivatives of poly(*p*-phenylene vinylene), PPV, has been studied via internal field emission[4], internal photoemission[5], electrochemical doping (cyclovoltammetric spectroscopy)[6] and photoelectron spectroscopy[7]. The data indicate that the π*-band and the top of the π-band are at ~3 eV and ~5 eV respectively, with respect to the vacuum. Thus, relatively good hole and electron injection can be achieved by using transparent indium-tin oxide (ITO) as the anode and calcium (Ca) or barium (Ba) as the cathode[2,4]. However, hole injection is very sensitive to the quality of the ITO. We have found that a layer (~30 nm) of conducting polyaniline[8], polypyrrole[9], or poly(ethylene-dioxythiophene)[10] provides excellent, reproducible hole-injecting contacts[8–10].

Figure 1 shows the external quantum efficiency for electroluminescence, QE_{ext}(EL), as a function of film thickness for two closely related PPV derivatives; OC1C10-PPV and MEH-PPV. The oscillatory dependence on the thickness (d) of the polymer layer arises from the proximity of the metallic mirror electrode; the emitting oscillator interacts with a virtual image oscillator "behind the mirror"[11,12]. Because the radiation from the emitter and the retarded radiation from the image oscillator interfere, the PL decay rate is an oscillatory function of the distance from the mirror. Consequently, for a thin film, the quantum yields for PL and EL are oscillatory functions of d. When the average distance from the mirror to the oscillator is too small ($d \ll 100$ nm), the losses from the metallic electrode quench the luminescence.

Blom *et al.* suggested that a high density of electron traps inhibits electron transport and prevents the achievement of balanced injection[13–15]. In an attempt to address this problem, we have studied the effect of blending electron transport materials into the conjugated polymer. The best results were obtained with (2-(4-biphenyl)-5-(4-tert-butylphenyl)1,3,4-oxidiazole, Bu-PBD, which was blended into the EL polymer at various concentrations. The butylphenyl substitution in Bu-PBD leads to good compatibility with the alkoxy-PPVs.

The light-emitting diodes (LEDs) were sealed with a glass cover that enables extended lifetimes at elevated temperatures. The external quantum efficiencies for PL and EL were directly compared for the OC1C10-PPV plus Bu-PBD blends in the LED configuration. For measurements of the EL efficiency, the external emission, integrated over all directions, was collected with a calibrated integrating sphere (at room temperature). PL efficiency measurements on the identical devices used the same integrating sphere[16]. For PL measurements, the excitation source was a monochromatic

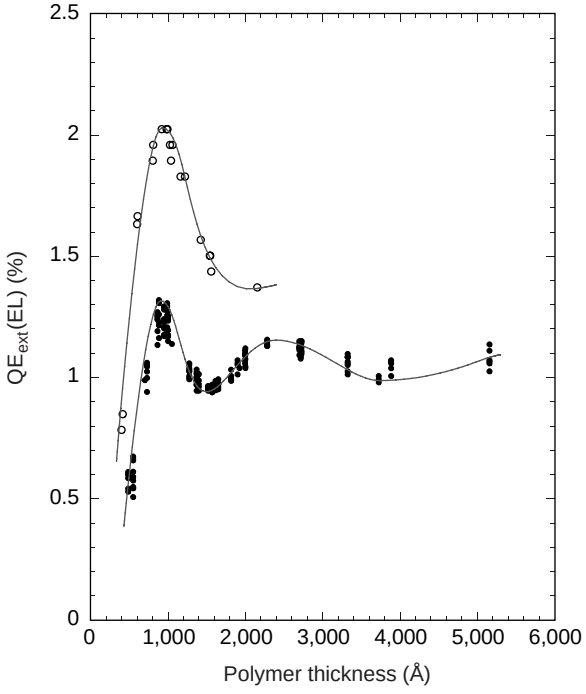

Figure 1 External electroluminescence quantum efficiency, QE_{ext}(EL), as a function of film thickness. Data are shown for two closely related alkoxy derivatives of poly(*p*-phenylene vinylene): OC1C10-PPV and MEH-PPV. The data from OC1C10-PPV [poly(2-(3,7-dimethyloctyloxy)-5-(2′-methoxy-1,4-phenylene vinylene)] form the upper curve (open circles); the data from MEH-PPV [poly(2-methoxy-5-(2′-ethylhexyloxy)-1,4-phenylene vinylene)] form the lower curve (filled circles). QE_{ext}(EL) in given in per cent; 1% ≡ 10^{-2} photons per carrier. The solid curves are guides to the eye.

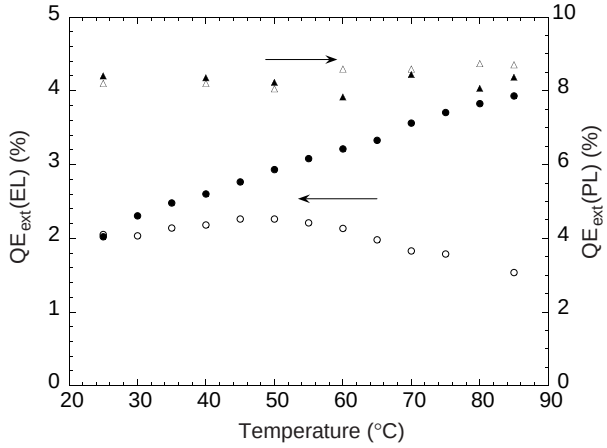

Figure 2 Temperature dependence of QE_{ext}(EL) and QE_{ext}(PL). Filled circles, QE_{ext}(EL) of a device fabricated from OC1C10-PPV plus 20% Bu-PBD. Data from an identical device fabricated with pure OC1C10-PPV (without Bu-PBD) are shown for comparison (open circles). The EL data were obtained at 6.7 mA cm^{-2}. Temperature dependences of the PL are also shown: pure OC1C10-PPV, open triangles; OC1C10-PPV plus 20% Bu-PBD, filled triangles.

laser beam (wavelength 488 nm) incident perpendicular to the plane of the device from the glass/ITO side. Extension of the external quantum efficiency measurements, PL and EL, to elevated temperatures used a photodiode that was carefully calibrated by the integrating sphere. By making the PL and EL measurements with the same device, the PL and EL data are compared in the same film and with the same electrodes. Using the device configuration simplifies the determination of the ratio of quantum efficiencies. Initially ignoring possible differences in recombination zones for PL and EL, the loss factors which contribute to both PL and EL divide out; both are subjected to quenching by proximity to the electrodes and to losses from internal reflection (and waveguiding), scattering and absorption. Thus, identical ratios are expected for the internal and external QE(EL)/QE(PL).

Figure 2 shows the temperature dependence of the external quantum efficiency for electroluminescence, $QE_{ext}(EL)$, of a device fabricated from a blend of OC1C10-PPV containing 20% (by weight) Bu-PBD (film thickness 100 nm). The data from an identical device fabricated with pure OC1C10-PPV (without Bu-PBD) are shown for comparison. For devices with Bu-PBD, QE_{ext} increases with temperature; at 85 °C, $QE_{ext}(EL)$ is twice that obtained at room temperature (for devices made without Bu-PBD, $QE_{ext}(EL)$ decreases slightly with temperature). The increase in QE_{ext} is unambiguous; measurements were taken on more than 10 devices for each Bu-PBD concentration with excellent reproducibility. The increase with temperature is reversible. The increase is a function of the Bu-PBD content; the optimum is at ~20% Bu-PBD. At higher concentrations, black spots are observed, indicative of phase separation.

The increase in $QE_{ext}(EL)$ does not result from an increase in the external quantum efficiency for photoluminescence, $QE_{ext}(PL)$; as shown in Fig. 2, the latter is temperature independent between room temperature and 85 °C in devices fabricated with and without the Bu-PBD. The temperature dependence of the operating voltage (for example, the voltage at 6.67 mA cm^{-1}) is the same for devices fabricated with and without Bu-PBD. Thus, the increase in QE_{ext} is not related to a change in mobility with temperature. This conclusion was confirmed by the observation that a bilayer device (an 8-nm layer of Bu-PBD deposited on top of OC1C10-PPV) showed a similar (though somewhat smaller) increase in QE_{ext} with temperature. Thus, the effect of the Bu-PBD is evidently to fine-tune the balance of the electron and hole injection. In this context, we note that the acceptor level in Bu-PBD is close in energy to the bottom of the π^*-band of the luminescence polymer[17].

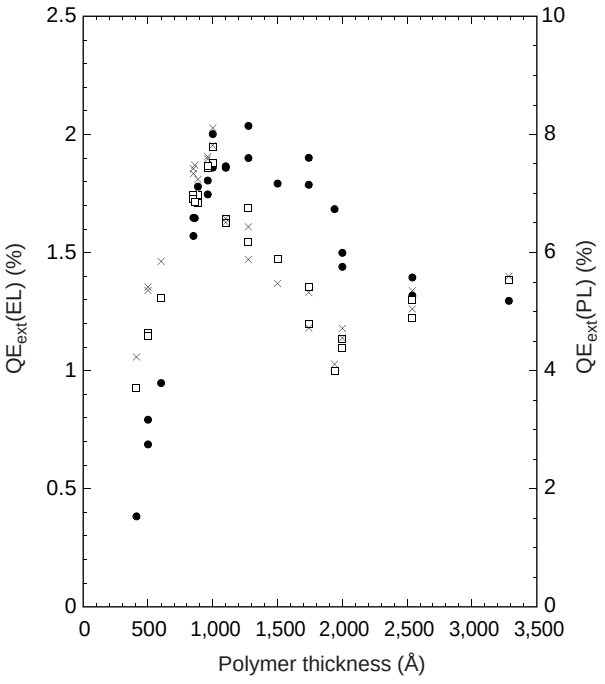

Figure 3 Comparison of external $QE_{ext}(EL)$, filled circles, with $QE_{ext}(PL)$, for devices with different luminescent polymer thickness. Open squares, PL efficiency as obtained when the incident light intensity was corrected by directly measuring the sum of unabsorbed and reflected light for each individual device outside the integrating sphere. Crosses, PL efficiency as obtained when the incident light intensity was corrected by measuring transmittance and reflectance of EL polymer films of different thickness on the glass substrate, following the procedure of Greenham *et al.*[16]

The PL and EL efficiencies were carefully checked on each of a series of devices fabricated with OC1C10-PPV films with different thickness (Fig. 3). The EL data are consistent with those in Fig. 1. The PL and EL efficiencies track one another as d is varied. We conclude from our results (Figs 2 and 3) that the external EL quantum efficiency for LEDs fabricated from OC1C10-PPV plus Bu-PBD (100-nm-thick) reaches $(4.0 \pm 0.2) \times 10^{-2}$ photons per electron (that is, 4.0(±0.2)%) at 85 °C. The external PL quantum efficiency as obtained from OC1C10-PPV films, with and without the Bu-PBD, in identical devices is 8±(0.8)% at zero field. By using EL and PL data from the same devices (made with OC1C10-PPV plus 20% Bu-PBD) to minimize the error, we conclude that $QE_{ext}(EL)/QE_{ext}(PL) \approx 0.5$.

The data in Fig. 2 were taken at constant current density (6.67 mA cm^{-2}) with operating voltages of 3–4 V; that is, at electric fields of $(3–4) \times 10^5$ V cm^{-1}. Previous measurements have demonstrated field-induced quenching of the PL; at 4 V, the PL quantum efficiency is reduced by ~10% (refs 18, 19). Thus, for the OC1C10-PPV plus Bu-PBD devices at 85 °C, $QE_{ext}(EL)/QE_{ext}(PL) = 0.5$ is a lower limit.

The quantum efficiencies for PL and EL are reduced through quenching by proximity to the metal and ITO electrodes. Quenching of the PL was directly measured by comparing PL efficiencies of a polymer film with $d = 100$ nm on glass (17.4%), on ITO/glass (12.3%) and on ITO/glass with a metal cathode (8.3%). In each case, the measurements were made in an integrating sphere with the polymer excited through the glass substrate. The data indicate approximately equal reductions in PL efficiency from the two electrodes. Because of the high density of electron traps, the recombination zone for EL is expected to be closer to the cathode, consistent with images of LEDs in the surface cell configuration[20]. Greenham *et al.*[12,16] showed that the luminescence is quenched within ~30–40 nm of the cathode. Quenching in the 30-nm-layer adjacent to the cathode was confirmed by analysis of the device characteristics[13–15]. Because of the spatially shifted recombination zones, the EL efficiency falls more rapidly than the PL efficiency as the thickness is reduced below 100 nm (Fig. 3). Consequently, the conclusion that $QE_{ext}(EL)/QE_{ext}(PL) \approx 0.5$ at 85 °C is conservative; the EL efficiency suffers a greater reduction from electrode quenching than the PL efficiency.

Because of the total internal reflection only a fraction $(1/2n^2$, where $n \approx 1.7$ is the index of refraction of the polymer) is emitted through the substrate[21]. That fraction of the emitted radiation which is waveguided is partially lost as a result of self-absorption in the polymer and, more importantly, as a result of losses in the metal cathode and the semitransparent anode. Consequently, the external quantum efficiencies are smaller than the internal quantum efficiencies. We find $QE_{ext}(PL) \approx 8\%$ in the device configuration in comparison with $QE_{int}(PL) \approx 15–20\%$, as obtained from direct measurements of the PL efficiency of OC1C10-PPV using the method of Greenham *et al.*[16] Thus, the measured reduction factor is approximately 2–2.5, less than the predicted value $(2n^2 \approx 6)$. We conclude that some of the light which is waveguided along the film/substrate emerges into the integrating sphere through a combination of surface scattering and emission from the edges.

The external PL and EL quantum efficiencies of OC1C10-PPV blended with Bu-PBD have been quantitatively compared. The ratio of the EL and PL external efficiencies, $QE_{ext}(EL)/QE_{ext}(PL) \approx 0.5$, is well beyond the theoretical limit for strongly bound singlet and triplet excitons. A summary and discussion of the magnitude of the exciton binding energy in semiconducting polymers has recently been published; values range from less than 0.1 eV to as high as 1 eV (ref. 22). Efficient triplet-to-singlet conversion (for example, by triplet–triplet annihilation) before non-radiative recombination (with subnanosecond decay time) is unlikely in hydrocarbon polymers where the spin-orbit coupling is weak. Thus, the high value for QE(EL)/QE(PL) indicates either that the exciton binding energy is small or that the cross-section for an electron–hole pair to form a singlet bound state is significantly higher than the cross-section to form a triplet. Evidence of photogenerated triplet excitations has been reported (ref. 23 and references therein). However, the relevant timescale was in the millisecond regime or longer; hence, the observed triplets might be defect-stabilized.

Our results indicate that QE(EL)/QE(PL) can be large in polymer LEDs. The goal is to achieve balanced injection with high electron and hole currents in materials with large QE(EL). As high PL efficiencies (>60%) have been demonstrated[24], the achievement of efficient EL emission from polymer LEDs should be possible. □

Received 15 April; accepted 12 November 1998.

1. Burroughes, J. H. *et al.* Light-emitting diodes based on conjugated polymers. *Nature* **347,** 539–541 (1990).
2. Braun, D. & Heeger, A. J. Visible light emission from semiconducting polymer diodes. *Appl. Phys. Lett.* **58,** 1982–1984 (1991).
3. Bradley, D. D. C. Conjugated polymer electroluminescence. *Synth. Met.* **54,** 401–415 (1993).
4. Parker, I. D. Carrier tunneling and device characteristics in polymer light-emitting diodes. *J. Appl. Phys.* **75,** 1656–1666 (1994).
5. Campbell, I. H., Hagler, T. W., Smith, D. L. & Ferraris, J. P. Direct measurement of conjugated polymer electronic excitation energies using metal/polymer/metal structures. *Phys. Rev. Lett.* **76,** 1900–1903 (1996).
6. Richter, M. M., Fan, F., Klavetter, F., Heeger, A. J. & Bard, A. Electrochemistry and electrogenerated chemiluminescence of films of the conjugated polymer 4-methoxy-(2-ethylhexyloxy)-2,5-polyphenylenevinylene. *Chem. Phys. Lett.* **226,** 115–120 (1994).
7. Brom, P., Birgersson, J., Johansson, N., Logdland, M. & Salaneck, W. R. Calcium electrodes in polymer LEDs. *Synth. Met.* **74,** 179–181 (1995).
8. Yang, Y., Westerweele, E., Zhang, C., Smith, P. & Heeger, A. J. Enhanced performance of polymer light-emitting diodes using high-surface area polyaniline network electrodes. *J. Appl. Phys.* **77,** 694–698 (1995).
9. Gao, J., Heeger, A. J., Lee, J. Y. & Kim, C. Y. Soluble polypyrrole as the transparent anode in polymer light-emitting diodes. *Synth. Met.* **82,** 221–223 (1996).
10. Cao, Y., Yu, G., Zhang, C., Menon, R. & Heeger, A. J. Polymer light-emitting diodes with polyethylene dioxythiophene-polystyrene sulfonate as the transparent anode. *Synth. Met.* **87,** 171–174 (1997).
11. Kuhn, H. Classical aspects of energy transfer in molecular systems. *J. Chem. Phys.* **53,** 101–108 (1970).
12. Greenham, N. C. Understanding the limits to performance in electronic devices based on PPV. *Bull. Am. Phys. Soc.* **43 (1),** 14 (1998).
13. Blom, P. W. M., de Jong, M. J. M. & Vleggaar, J. J. M. Electron and hole transport in poly(p-phenylene vinylene). *Appl. Phys. Lett.* **68,** 3308–3310 (1996).
14. Blom, P. W. M., de Jong, M. J. M. & Munster, M. G. Electric-field and temperature dependence of the hole mobility in poly(p-phenylene vinylene). *Phys. Rev. B* **55,** 656–659 (1997).
15. Blom, P. W. M., de Jong, M. J. M. & Breedijk, S. Temperature dependence electron-hole recombination in polymer light-emitting diodes. *Appl. Phys. Lett.* **71,** 930–932 (1997).
16. Greenham, N. C. *et al.* Measurement of absolute photoluminescence quantum efficiencies in conjugated polymer. *Chem. Phys. Lett.* **241,** 89–96 (1995).
17. Schmidt, A., Anderson, M. L. & Armstrong, N. R. Electronic states of vapor deposited electron and hole transport agents and luminescent materials for light-emitting diodes. *J. Appl. Phys.* **78,** 5619–5625 (1995).
18. Kersting, R. *et al.* Ultrafast field-induced dissociation of excitons in conjugated polymers. *Phys. Rev. Lett.* **73,** 1440–1443 (1994).
19. Moses, D. *et al.* Mechanism of carrier generation in poly(phenylene vinylene): Transient photoconductivity and photoluminescence at high fields. *Phys. Rev. B* **54,** 4748–4754 (1996).
20. Greenham, N. C., Friend, R. H. & Bradley, D. D. C. Angular dependence of the emission from a conjugated polymer light-emitting diode: implications for efficiency calculations. *Adv. Mater.* **6,** 491–494 (1994).
21. Lemmer, U. *et al.* Electroluminescence from poly(phenylene vinylene) in a planar metal-polymer-metal structure. *Appl. Phys. Lett.* **68,** 3007–3009 (1996).
22. Sariciftci, N. S. (ed.) *Primary Photoexcitations in Conjugated Polymers: Molecular Excitons vs Semiconductor Band Model* (World Scientific, Singapore, 1997).
23. Smilowitz, L. & Heeger, A. J. Photoinduced absorption from triplet excitations in poly(2-methoxy,5-(2′-ethylhexyloxy)-p-phenylene vinylene) oriented by gel processing in polyethylene. *Synth. Met.* **48,** 193–196 (1992).
24. Hide, F. *et al.* Semiconducting polymers: a new class of solid state laser materials. *Science* **273,** 1833–1836 (1996).

Acknowledgements. Research at UNIAX was partially supported by the Office of Naval Research.

Correspondence and requests for materials should be addressed to A.J.H.

Hybrid hydrogels assembled from synthetic polymers and coiled-coil protein domains

Chun Wang*, Russell J. Stewart* & Jindřich Kopeček*†

*Departments of * Bioengineering and † Pharmaceutics and Pharmaceutical Chemistry, University of Utah, Salt Lake City, Utah 84112, USA*

Stimuli-sensitive polymer hydrogels, which swell or shrink in response to changes in the environmental conditions, have been extensively investigated and used as 'smart' biomaterials and drug-delivery systems[1,2]. Most of these responsive hydrogels are prepared from a limited number of synthetic polymers and their derivatives, such as copolymers of (meth)acrylic acid, acrylamide and *N*-isopropyl acrylamide[3–12]. Water-soluble synthetic polymers have also been crosslinked with molecules of biological origin, such as oligopeptides[13] and oligodeoxyribonucleotides[14], or with intact native proteins[15]. Very often there are several factors influencing the relationship between structure and properties in these systems, making it difficult to engineer hydrogels with specified responses to particular stimuli. Here we report a hybrid hydrogel system assembled from water-soluble synthetic polymers and a well-defined protein-folding motif, the coiled coil. These hydrogels undergo temperature-induced collapse owing to the cooperative conformational transition of the coiled-coil protein domain. This system shows that well-characterized water-soluble synthetic polymers can be combined with well-defined folding motifs of proteins in hydrogels with engineered volume-change properties[16,17].

The coiled coil[18], a left-handed superhelix of two or more right-handed α-helices, has been identified in proteins ranging from

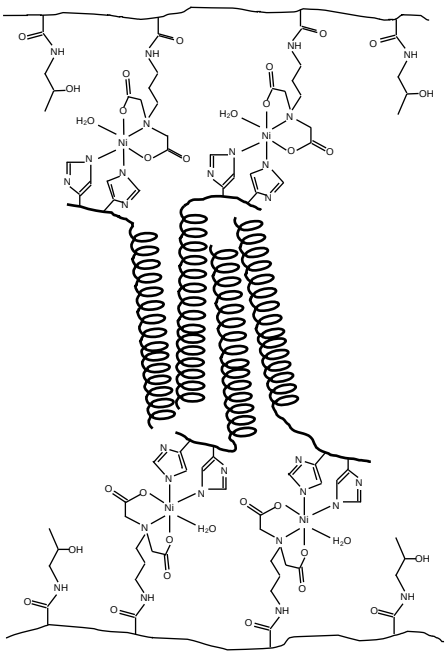

Figure 1 Structural representation of the hybrid hydrogel primary chains and the attachment of His-tagged coiled-coil proteins. Poly(HPMA-co-DAMA) is shown here as the primary chains. The pendant iminodiacetate groups form complexes with transition-metal ions, such as Ni^{2+}, to which the terminal histidine residues of the coiled coils are attached. A tetrameric coiled coil (not drawn to scale), consisting of two parallel dimers associating in an antiparallel fashion, is shown here as an example of many of the possible conformations.